U

ULTRAVIOLET RADIATION

In general scientific usage, *ultraviolet radiation* refers to radiant emissions in that portion of the electromagnetic spectrum between X-rays and visible radiation, i.e. in the wavelength range 0.01–0.4 μm approximately. However, outside the Earth's atmosphere, 99% of the solar irradiance occurs in the spectral range 0.15–4 μm; hence, climatologically significant ultraviolet radiation is that lying between 0.15 μm and 0.4 μm in the spectrum, a band containing about 9% of the radiant energy of solar origin prior to atmospheric attenuation. Solar ultraviolet radiation is conventionally subdivided into three wavelength bands, based primarily on potential biological activity: UV-A (0.32–0.4 μm), UV-B (0.28–0.32 μm), and UV-C (< 0.28 μm).

Radiation with wavelengths shorter than 0.21 μm (most of the UV-C) is absorbed by oxygen and nitrogen in processes of ionization, dissociation, and heating at elevations in excess of 80 km in the thermosphere and ionosphere. However, most absorption takes place in the stratosphere, where ozone absorbs radiation in the wavelength range 0.21–0.31 μm. Collectively, these attenuation processes reduce the solar irradiance at the surface by only about 3% on a global, annual basis. Nevertheless, ozone's absorption of ultraviolet radiation to a large extent maintains the temperature structure of the stratosphere. As a result, solar radiation at the Earth's surface lacks UV-C and is deficient in UV-B, possessing little radiant energy at wavelengths shorter than 0.31 μm.

Large percentage fluctuations have been detected in the monochromatic irradiance received outside the atmosphere at ultraviolet wavelengths, primarily associated with solar activity. Because the magnitude of these fluctuations is greatest at the extreme short end of the solar ultraviolet, and decreases with increasing wavelength, the effect on the spectrally integrated solar irradiance is small (probably less than 0.1%). However, changes in stratospheric warming resulting from irradiance fluctuations in the far ultraviolet have been linked to dynamic processes occurring in the troposphere by some authors, and speculation has ensued that longer-term variations in ultraviolet emissions by the sun may be responsible for climate changes.

Concern has been expressed about the role of stratospheric ozone depletion, brought about by the introduction of chlorofluorocarbons and other byproducts of human activity into the atmosphere, in increasing UV-B irradiances at ground level. Ultraviolet radiation, particularly at wavelengths shorter than 0.3 μm, has strong actinic effects, and excessive exposure to such radiation has been linked to sunburn, skin cancer, and eye disease in humans. Deleterious effects on terrestrial and marine ecosystems also have been suggested, as well as the potential for adverse effects on air quality. Nevertheless, this radiation possesses beneficial attributes such as forming vitamin D in the skin and devitalizing bacteria and similar microorganisms of disease.

A. John Arnfield

Bibliography

Kemp, D.D., 1994. *Global Environmental Issues: A Climatological Approach*. New York: Routledge.

Liou, K.N., 2002. *An Introduction to Atmospheric Radiation.* New York: Academic Press.

Paltridge, G.W., and Platt, C.M.R., 1976. *Radiative Processes in Meteorology and Climatology.* New York: Elsevier.

United Nations Environment Programme, 2003. *Environmental Effects of Ozone Depletion and its Interactions with Climate Change*: 2002 Assessment. Nairobi: UNEP.

Cross-references

Energy Budget Climatology
Electromagnetic Radiation
Ozone
Seasonal Affective Disorder
Sunspots

UNITS AND CONVERSIONS

The strength and utility of a measurement system depends on the existence of a consistent set of units and standards around which a complete system can develop. These fundamental standards of weights and measures are maintained on a federal level in the United States by the National Bureau of Standards. On a worldwide level the International Bureau of Weights and Measures in Paris, which was established by the Treaty of Meter in 1875, sets the standard.

The Treaty of Meter also provided for an International Conference of Weights and Measures to meet at regular intervals. In 1957 this conference changed the world standard of length from the platinum–iridium meter bar to a multiple (1 650 763.73) of the wavelength of orange-red light of krypton 86. This new wavelength standard has several advantages over the metal one. It is indestructible, immutable, a constant of nature, and can be reproduced anywhere in the world with an accuracy of one part in one hundred million. In 1960 this same conference adopted an International System of Units (abbreviated SI for Système International). The SI is a metric system based on seven fundamental physical quantities in terms of which all others are to be defined so as to be consistent with the generally accepted equations of physics. These quantities and their units are mass (kilogram), length (meter), time (second), temperature (Kelvin), current (ampere), and luminous intensity (candela). The seventh unit, the mole, was adopted in 1971.

The SI supplants the older cgs and mks systems, although they are still the two most commonly used. In the United States the customary system still employed by established tradition uses the foot, pound, and second; these are defined in terms of the SI units by simple numerical ratios. This customary system, inherited from Britain, is widely used in industry and commerce in both the United States and much of the English-speaking world, but it is not inherently consistent and is little used for strictly scientific measurements. Certain units of measurement, e.g. the nautical mile, which is equivalent to one degree of latitude, have such obvious value that it will be difficult to replace them.

Metric units of measurement

In the metric system of measurement, designations of multiples and subdivisions of any unit may be arrived at by combining with the name of the unit the prefixes deka, hecto, and kilo meaning, respectively, 10, 100, and 1000, and deci, centi, and milli, meaning, respectively, one-tenth, one-hundredth, and one-thousandth. In certain cases, particularly in scientific usage, it becomes convenient to provide for multiples larger than 1000 and for subdivisions smaller than one-thousandth. Accordingly, the following prefixes have been introduced and these are now generally recognized:

yotta (Y), meaning 10^{24}	deci (d), meaning 10^{-1}
zetta (Z), meaning 10^{21}	centi (c), meaning 10^{-2}
exa (E), meaning 10^{18}	milli (m), meaning 10^{-3}
peta (P), meaning 10^{15}	micro (μ), meaning 10^{-6}
tera (T), meaning 10^{12}	nano (n), meaning 10^{-9}
giga (G), meaning 10^{9}	pico (p), meaning 10^{-12}
mega (M), meaning 10^{6}	femto (f), meaning 10^{-15}
kilo (k), meaning 10^{3}	atto (a), meaning 10^{-18}
hecto (h), meaning 10^{2}	zepto (z), meaning 10^{-21}
deka (da), meaning 10^{1}	yocto (y), meaning 10^{-24}

These prefixes increasingly are used with data exchanges. The bit (b) and byte (B) are the standard unit of data quantity, and Gb, MB and GB are commonly used.

Time

Second: the standard unit of time. It was originally defined as 1/86 400 of a mean solar day, but the standard was changed in 1960 by the Eleventh General Conference on Weights and Measures to be 1/31 556 925.9747 of the tropical year 1900. The second is the duration of 9 192 631 770 periods of the radiation corresponding to the transition between the two hyperfine levels of the ground state of the cesium 133 atom. The present standard avoids the variability caused by changes in the Earth's period of rotation about its axis.

1 minute = 60 seconds
1 hour = 3600 seconds
1 sidereal month = 27.32167 days
1 synodical month = 29.53059 days
1 tropical (ordinary) year = 31 556 925.9747 seconds
1 calendar year (common) = 31 536 000 seconds

Temperature

Temperature: a term used to express the relative intensity of heat. It is identified with the kinetic energy of translation of molecules and, in accordance with the kinetic theory of gases, has an absolute zero where all motion has ceased. It is also an aspect of matter that governs the ability to transfer heat from or to other matters. Heat will not transfer between two bodies if they are at the same temperature. There are three temperature scales currently employed: the Fahrenheit scale, the Centigrade (Celsius) scale, and the Kelvin scale. By international agreement, Celsius is favored over Centigrade, but the latter is still widely preferred.

Temperature scales – Centigrade (Celsius) to Fahrenheit

Equivalents
1 C° = 1.8 F°
1 F° = 0.5556 C°
1 K (Kelvin) = 1 C° −273°C = −459.4°F = 0°K

Conversion formulas
°F = 9/5°C + 32
°C = 5/9 (°F −32)

Note: °F is read "degrees Fahrenheit"
F° is read "Fahrenheit degrees"
°C is read "degrees Centigrade or Celsius"
C° is read "Centigrade or Celsius degrees"

1°F per foot = 0.0182269°C per centimeter
1°C per centimeter = 54.864°F per foot
1 ft per °F = 0.54864 m per °C
1 m per °C = 1.82269 ft per °F

Mass and weight

Gram: the unit of mass in the metric system that was first defined to be equal to the mass of a cubic centimeter of pure

water at the temperature of its maximum density (4°C). A platinum cylinder was made, known as the kilogram, and declared to be the standard for 1000 grams.

Gram-atomic weight: the atomic weight of an element expressed in grams, customarily based on a scale on which the gram-atomic weight of oxygen is 16 000 grams, but more precisely, based on a scale on which the gram-atomic weight of carbon 12 is 12 000. The gram-atomic weight of all elements contains the same number of atoms. This number, called Avogadro's number, is 6.032×10^{23} and is termed a gram atom.

Gram-equivalent weight: the equivalent weight of an element of compound expressed in grams, customarily based on a scale on which the equivalent weight of oxygen is 8000 grams. It is the gram-atomic weight of an element (or formula weight of a radical) divided by the absolute value of its valence (oxidation state).

Gram-molecular weight: the molecular weight of an element or compound expressed in grams. The gram-molecular weight of all elements or compounds contains the same number of molecules, 6.032×10^{23} (Avogadro's number), and is termed one mole.

Ton: in the United States a ton is a unit of weight equal to 2000 pounds, commonly called a short ton. The long ton, more widely used in England, is equal to 2240 pounds. The metric ton is equal to 1000 kilograms.

1 short ton = 0.90718 metric ton = 0.892857 long ton
1 long ton = 1.12 short tons = 1.016047 metric tons
1 metric ton = 0.984207 long ton = 1.10232 short tons
1 pound (avoirdupois) = 7000 grains = 16 ounces
1 ounce (av.) = 437.5 grains
1 ounce (troy) = 480 grains
1 pound (troy) = 5760 grains
1 ounce (apothecaries) = 480 grains
1 kg = 10^3 g = 2.20462 lb
1 lb = 0.453592 kg = 453.592 g

Linear measures

Meter: the standard unit of length in the metric system. It was first defined by a platinum end standard, the meter of the archives, in Paris. This length, based on a measure of an arc from Dunkirk, France, to Montzuich, Spain, was to be one ten-millionth part of the meridional quadrant of the Earth. In 1889 at the first general conference of the International Bureau of Weights and Measures, the meter was redefined in terms of the platinum–iridium bar known as the international prototype meter at the international bureau. This standard meter is now defined as 1 650 763.73 times the wavelength in a vacuum of krypton 86.

The *micron* is a unit of length equal to 10^{-6} meters. It is commonly employed in the measure of short distances such as the wavelength of light and is represented by the Greek letter μÅThe Angstrom unit (Åis also used for wavelengths; one Å = 10^{-10} m.

Mile: the mile most commonly used in English-speaking countries is the English or statute mile of 5280 feet. This distance was supposedly designated by 1000 paces of the Roman Legions stationed in Britain. Navigators use the nautical mile, which was originally defined as the length of one minute of arc on a great circle drawn on the surface of a sphere with the same area as the Earth. This length is 6080.27 feet. However, since the Earth is an oblate spheroid flattened at the poles, the length of one minute of arc measured along a meridian varies in different latitudes. It is shortest near the poles and longest near the equator with an average length of 6077.015 feet. To resolve this confusion, an international agreement was made defining the nautical mile as 1852 meters, the present value of the international nautical mile. The United States nautical mile, equal to 1.00067387 international nautical miles, and the British nautical mile, equal to 1.00063931 international nautical miles, are occasionally used.

Foot: a unit of length used in the British system of units and employed in English-speaking countries. It was originally standardized in England in 1870 as one-third the length of a yard. In 1959 the foot was defined as 0.3048 meter in accordance with an agreement among the directors of the standards laboratories of English-speaking countries. As a linear measure the foot is of great antiquity, originally identified as the length of a man's foot.

Yard: the fundamental distance in the English measuring system is taken as the distance at 62°F between two fine lines on gold plugs in a bronze bar at Westminster, England, known as the Troughton scale. In 1893 the yard was redefined as 3600/3937 meter.

1 cm = 0.39370 in = 0.032808 ft
1 km = 10^5 cm = 0.62137 mile
1 fathom = 6 ft = 1.8288 m
1 nautical mile = 1.85325 km
1 in = 2.54001 cm
1 ft = 30 480 cm
1 statute mile = 1.60935 km = 5280 ft
1 astronomical unit = 1.496×10^8 km = 92 957 000 miles
1 light year = 9460×10^{12} km = 5.878×10^{12} miles
1 parsec = 3.085×10^{13} km = 1.917×10^{13} miles

Metric to English units – equivalents of length
1 micron (μ) = 0.001 millimeter (mm) = 0.00004 inch (in)
1 mm = 0.1 centimeter (cm) = 0.03937 in
1000 mm = 100 cm = 1 meter (m) = 39.27 in = 3.2808 feet (ft)
1 m = 0.001 kilometer (km) = 1.0936 yards (yd)
1000 m = 1 km = 0.62137 mile
1 in = 2.54 cm
12 in = 1 ft = 0.3048 m

Square measures

1 square ft = 0.00002295684 acre
1 acre = 43 560 ft^2 = 0.0015625 $mile^2$
1 square yard = 0.836127 m^2
1 hectare = 2.471054 acres
1 square mile (statute) = 640 acres
1 square cm = 0.1550 square in = 0.0010764 square ft
1 square km = 10^{10} square cm = 0.3861 square mile
1 square in = 6452 square cm
1 square ft = 929.0 square cm
1 square mile = 2.5900 square km
1 mm^2 = 0.00155 in^2 1 in^2 = 6.452 cm^2
1 m^2 = 10.764 ft^2 1 ft^2 = 0.09290 m^2
1 km^2 = 0.3861 $mile^2$ 1 $mile^2$ = 2.5900 km^2

Cubic measures

1 gal (UK) = 4.5461 liters = 1.200956 gal (US)
1 liter = 0.219969 gal (UK) = 0.264173 gal (US)

1 gal (US) = 3.7854 liters = 0.832670 gal (UK)
1 cc = 0.0610 cu in = 0.000035314 cu ft
1 cu in = 16.387 cc
1 cu ft = 28 317 cc
1 mm^3 = 0.000061 in^3 1 in^3 = 16.387 cm^3 (cc)
1 cm^3 (cc) = 0.0610 in^3 1 ft^3 = 0.028317 m^3
1 m^3 = 35.315 ft^3 1 $mile^3$ = 4.1681 km^3
1 km^3 = 0.239911 $mile^3$

Velocity

1 knot = 51.4 cm/s
1 ft/s = 30.480 cm/s = 1.0973 km/h
1 mi/h = 1.6093 km/h = 44.704 cm/s
1 cm/s = 3.728×10^{-4} mile/min = 0.02237 mile/h
1 km/h = 27.7778 cm/s
1° ψ per day = 1.2863 m/s = 2.8774 mile/h = 2.4987 knots

Force

As units of force, frequency gram weight, kilogram weight, pound weight, etc., are used. We denote them here by g*, kg*, and lb*.

1 dyne = 0.0010197 g* = 2.2481×10^{-6} lb* = 1 g/s^2
1 megadyne = 10^6 dynes
1 g* = 980.665 dynes
1 kg* = 980.665×10^3 dynes
1 lb* = 4.4482×10^5 dynes

Pressure

The SI unit of pressure is the pascal, symbol Pa, the special name given to a pressure of one newton per square metre (N/m^2). The relationships between the pascal and some other pressure units are shown in Table U1, but note that not all are, or can be, expressed exactly.

Following the Eighth Congress of the World Meteorological Organization in 1986, the term hectopascal (hPa) is preferred to the numerically identical millibar (mb) for meteorological purposes. This choice was made, despite the fact that hecto ($\times$ 100) is not a preferred multiple in the SI system.

The so-called "manometic" pressure unit definitions such as millimeters of mercury and inches of mercury depend on an assumed liquid density and acceleration due to gravity, assumptions which inherently limit knowledge of their relationship with the pascal. In order to encourage the demise of non-SI units, whose definitions are becoming inadequate for the most precise measurement of pressure, there is international effort to exclude them from conversion tables or, in the meantime, restrict the precision of newly published conversion factors.

Table U1 Units of pressure

Unit	Symbol	No. of pascals
bar	bar	1×10^5
millibar	mb	100
hectopascal	hPa	100
conventional millimeter of mercury	mmHg	133.322...
conventional inch of mercury	inHg	3 386.39...
torr	torr	10 1325/760
pound-force per square inch	lbf/in^2	6 894.76...

The torr is defined as exactly 101325/760 Pa – the "760" coming from the original and arbitrary definition of standard atmosphere. Its value differs from the conventional millimeter of mercury by about 1 part in 7 million.

Other pressure units and conversions include the following.

1 barye = 1 dyne/cm^2 = 9.8692×10^{-7} atmosphere = 10^{-6} bar = 1.4504×10^{-5} lb/sq in
1 bar = 10^6 baryes = 10^6 dynes/cm^2 = 0.98692 atmosphere = 14.504 lb/sq in = pressure of 750.06 mm of Hg
1 millibar = 10^{-3} = 10^3 dynes/cm^2 = pressure of 0.75006 mmHg
1 megabar = 10^6 bars
1 kg/cm^2 = 0.980665×10^6 dynes/cm^2 = 14.233 lb/sq in
1 lb/sq ft = 4.7254×10^{-4} atmosphere = 478.80 dynes/cm^2 = 47.880 newtons/m^2
1 lb/sq in = 0.068046 atmosphere = 0.068947 bar = 6.8947×10^4 dynes/cm^2 = 6894.8 newtons/m^2
1 atmosphere = 1.0332 kg/cm^2 = 1.01325 bars = 14.7 lb/sq in = pressure of 760 mmHg at 0°C and g = 980.665 cm/s^2

Energy–work

Foot candle: the unit of illumination in general use in the United States. This is defined as the illumination on an area, one foot square, on which there is a luminous flux of one lumen uniformly distributed. It may also be defined as the illumination on a surface of which all points are at a distance of one foot from a uniform point source of one candle.

Foot-lambert: a unit of luminance defined as the uniform luminance of a perfectly diffusing surface either emitting or reflecting light at the rate of one lumen per square foot. It may also be defined as $1/n$ candle per square foot and is sometimes referred to as the apparent foot-candle.

Foot-pound: a unit in the English gravitational system; it may be defined in two ways: (1) a unit of energy equal to the work done when one pound of force displaces a point to which the force is applied one foot in the direction of the applied force; (2) a unit of torque equal to the time-rate of change of angular momentum produced by a pound of force acting at a perpendicular distance of one foot from the axis of rotation.

Foot-poundal: a unit in the English absolute system; it may be defined either as a unit of energy, equal to the work done by a force of magnitude one poundal when the point at which the force is applied is displaced one foot in the direction of the force, or as a unit of torque equal to the time rate of change of angular momentum produced by a force of magnitude one poundal acting at a perpendicular distance of one foot from the axis of rotation.

Calorie: used in the cgs system, this unit represents the quantity of heat required to raise 1 gram of water through 1°C (at 15°C).

Kilocalorie: equal to 10^3 calories, this is often cited as a calorie in metabolic studies. This use has led to considerable confusion.

Langley: proposed in 1942 as a solar radiation unit. Initially given as calories per sq cm per minute, the time dimension was dropped in 1947. Thus 1 Langley = 1 cal/cm^2 = 697.8 W m^{-2}. The unit was named for S.P. Langley (1834–1906) of the Smithsonian Institution.

British thermal unit (BTU): the energy required to raise the temperature of one pound of water through 1°F (39° to 40°F).
1 erg = 1 dyne centimeter = 1 g cm^2/s^2
1 joule = 10^7 ergs = 0.102 m kg* = 0.737 ft-lb

1 gram calorie corresponds to 4.19×10^7 ergs
1 watt = 10^7 ergs per second = 1 joule per second
1 horsepower = 746 watts
British thermal unit (39°F) (Btu) = 1060.4 joules (absolute)
British thermal unit (60°F) (Btu) = 1054.6 joules (absolute)
Gram-calorie (mean) = 1.5593×10^{-6} horsepower

Energy flow representation

In attempting to standardize the representation of energy flow, the World Meteorological Organization (1971) suggests the following symbols:

$Q\downarrow$ ($Q\downarrow = K\downarrow + L\downarrow$)	Downward radiation
$K\downarrow$ ($K\downarrow = S + D$)	Global solar radiation
S	Vertical component of direct solar radiation
D	Diffuse solar radiation
$L\downarrow$ ($A\downarrow$)($L\downarrow = A\downarrow$)	Downward atmospheric radiation
$Q\uparrow$ ($Q\uparrow = K\uparrow + L\uparrow$)	Upward radiation
$K\uparrow$	Reflected solar radiation
R	Upward solar radiation reflected by Earth's surface alone
$L\uparrow$	Upward terrestrial radiation
Lq	Upward terrestrial radiation – surface
r	Reflected atmospheric radiation
$A\uparrow$	Upward atmospheric radiation
Q	Net radiation
K^*	Net solar radiation
L^*	Net terrestrial radiation

Given these symbols, components of the Earth's budget can be represented by equations. Of particular importance is net radiation.

Net radiation = Incoming − Outgoing

$$Q = Q\downarrow - Q\uparrow$$

$$\text{or } Q^* = K^* + L$$

$$\text{Since } K^* = K\downarrow - K\uparrow \text{ and } L^* = L\downarrow - L\uparrow$$

$$Q^* = (K\downarrow - K\uparrow) + (L\downarrow - L\uparrow)$$

alternatively

$$\text{Since } Q\downarrow = K\downarrow + L\downarrow \text{ and } Q\uparrow K\uparrow + L\uparrow$$

$$\text{then } Q^* = (K\downarrow + L\downarrow) - (K\uparrow + L\uparrow)$$

John E. Oliver

Bibliography

Brown, J.M., 1973. *Tables and Conversions for Microclimatology*. USDA Forest Service Technical Report NC-8. Washington, DC: US Government Printing Office.

Cardarelli, F., 1997. *Scientific Unit Conversion.* London: Springer-Verlag.

Carmichael, R.D., and Smith, E.R., 1962. *Mathematical Tables and Formulas*. New York: Dover.

Clark, S.E., Jr, (ed.), 1966. *Handbook of Physical Constants*, rev. edn. Geological Society of America Memorandum 97. Boulder, Co: Geological Society of America.

Clason, W.E. (comp.), 1964. *Elsevier's Lexicon of International and National Units*. New York: Elsevier.

Forsythe, W.E. (comp.), 1954. *Smithsonian Physical Tables*. Washington, DC: Smithsonian Institution.

Gilbert, J.A., 1967. Units, numbers, constants and symbols. In Fairbridge, R.W., ed., *The Encyclopedia of Atmospheric Sciences and Astrogeology*. New York: Reinhold.

Gray, D.E. (ed.), 1957. *American Institute of Physics Handbook*. New York: McGraw-Hill.

Hodgman, C.D. (ed.), 1960. *Handbook of Chemistry and Physics*. Cleveland, OH: Chemical Rubber Publishing Co.

Jeffreys, H., 1948. The figures of the Earth and of the Moon (3rd paper), *Royal Astonomical Society Monthly Notices*, **5**: 219–247.

Jerrard, H.G., and McNeill, D.B., 1980. *A Dictionary of Scientific Units*. London: Chapman & Hall.

Kayan, C.E. (ed.), 1959. *Systems of Units*, Publication No. 57. Washington, DC: American Association for the Advancement of Science.

National Physical Laboratory, United Kingdom. www.npl.co.uk

NIST References on Constants, Units and Uncertainties. http:.physics.nist.gov

McNish, A.G., 1957. Dimensions, units and standards. *Physics Today*, **10**: 19–25.

United Nations Studies in Methods, 1987. *Energy Statistics, Units of Measure and Conversion Factors*. Series F, No. 44. New York: United Nations.

World Meteorological Organization, 1971. *Guide to Meteorological Instruments and Observing Practices*, 4th edn. W.M.O. No. 8TP3. Geneva: World Meteorological Organization.

URBAN CLIMATOLOGY

Urbanization and climate

The process of urbanization significantly alters natural surface and atmospheric conditions. Oke, in Thompson and Perry (1997), suggests that urban atmospheres demonstrate the strongest evidence we have of the potential for human activities to change climate. In the twentieth century rapid urbanization has occurred on a worldwide scale and the majority of the world's population lives in cities. Rapid expansion of cities has produced concurrent alterations in the urban climatic environment (Landsberg, 1981).

In general there are many apparent anthropogenic impacts on our atmospheric environment (Changnon, 1983). These range from microscale (e.g. replacing trees with a parking lot) to macroscale (e.g. carbon dioxide effects on global climate by fossil fuel combustion and emissions). This discussion focuses on the causes of alterations in climate in urban areas. Processes are reviewed that are keys to the formation of an urban climate and the underlying energy, moisture, and air movement patterns that distinguish urban climates from their surroundings.

An extensive literature addresses the specific problem of air pollution on regional and global scales as it relates to general processes of urbanization. The field of urban climatology has developed to the level of theory and detailed investigations that we see today in part due to early interests in air quality in cities. This discussion, however, does not focus on air pollution effects *per se*. Urban climate can be understood, to a large degree, by the study of modifications which develop primarily through the effects of land-use changes and feedbacks into the energy, moisture, and local air motion systems. Air quality certainly plays a role. The following discussion is limited to micro-, local, and meso-scales. It is also restricted to processes taking place in what are called the urban canopy

layer (UCL – beneath roof level) and the urban boundary layer (UBL – extending from roof level to the height at which urban influences are absent; Oke, 1998, see Figure U1).

The first real growth of urban climatology dates from the 1920s, followed by rapid increases in interest in urban climates between the 1930s and 1960s (especially in Germany, Austria, France, and North America). After World War II, and into the environmental era of the 1960s and 1970s and beyond, there was an exponential increase in urban climatic investigations. Investigations have simultaneously become less descriptive, more oriented to quantitative and theoretical modeling, and more integrative and interdisciplinary (e.g. World Meteorological Organization, 1970; de Dear et al., 2000). There are many scholarly reviews of the subject and accompanying bibliographies that illustrate the overall problem of how cities alter their climatic environment (e.g. Brazel, 1987; Chandler, 1976; Beryland and Kondratyev, 1972; Landsberg, 1981; Lee, 1984; Oke, 1974, 1979, 1979, 1980; and in Bonan, 2002). Today, urban climatology has achieved its own recognition as a subdiscipline in climatology and among allied disciplines such

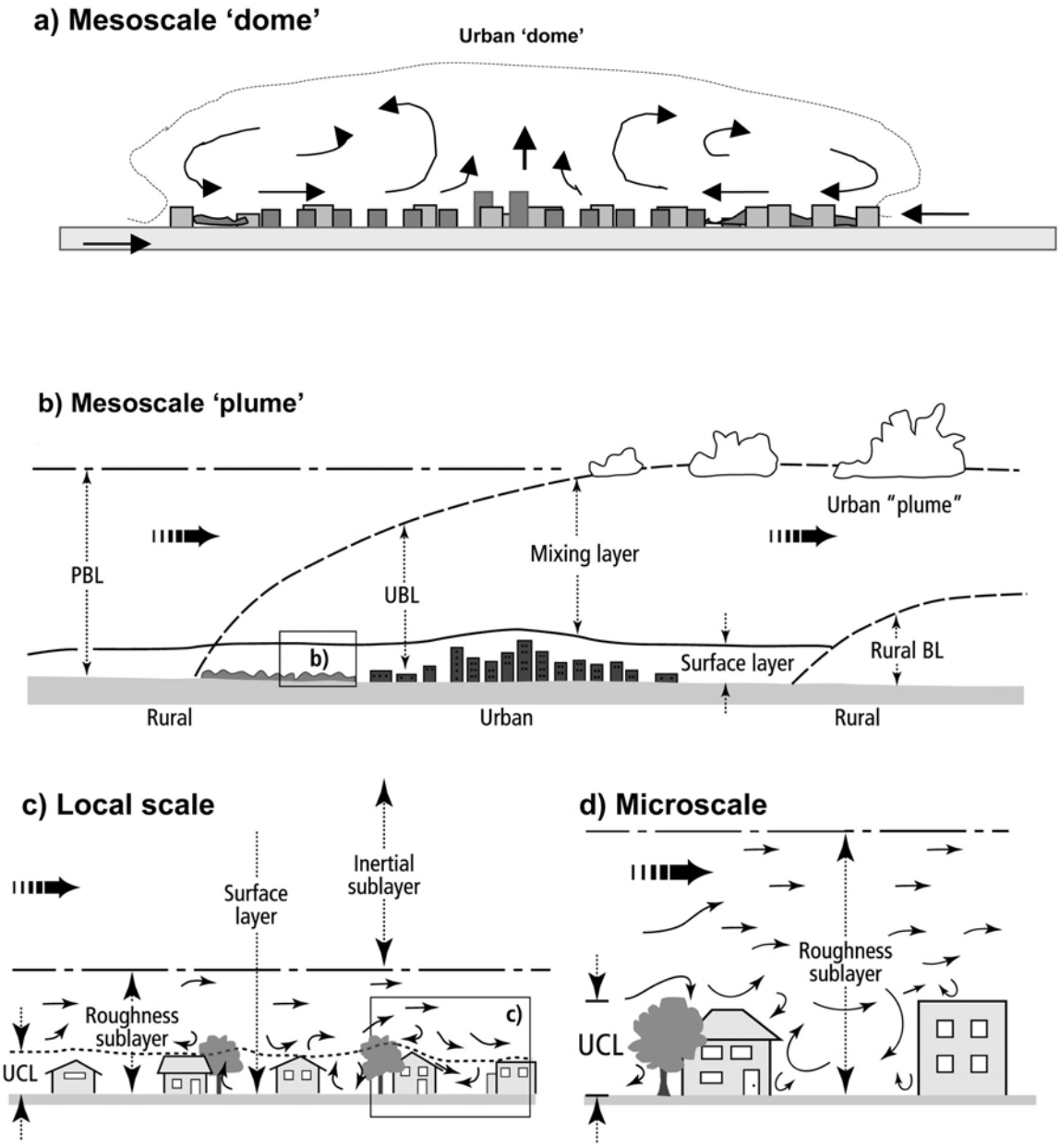

Figure U1 The idealized vertical structure of urban-modified air. (**a**) The whole city (mesoscale) in near-calm conditions with its "dome", and (**b**) in a steady regional air flow with its urban "plume". (**c**) A single urban terrain zone (local scale) showing the internal layering of the urban canopy (UCL) and lower portion of the urban boundary (UBL) layers. (**d**) A single street canyon (microscale) and building elements (after Oke, 1998).

as planning, ecology, environmental science, and meteorology (e.g. as evidenced in de Dear et al., 2000).

Factors controlling urban climates

Many aspects of urbanization change the physical environment and lead to alterations in energy exchanges, thermal conditions, moisture fluxes (evaporation, precipitation, and runoff) and wind circulation systems. These include: (1) air pollution, (2) anthropogenic heat, (3) surface waterproofing, (4) thermal properties of the surface materials, and (5) surface geometry (Oke, 1981). Other factors that must be considered relate to the setting of the city, such as relief, proximity to water bodies, size of the city, population density, and land-use distributions. Oke (1997) provides a summary of the typical resulting alterations of climatic elements in cities compared to rural environs (see Table U2).

The magnitude–frequency concept is important but less studied in urban climatology. How large are climatic alterations in a city and how often are they that large? The latter part of the question demands analysis of the linkages of microscale–mesoscale alteration magnitudes with more macroscale conditions, such as the role of synoptic climatology on urban climate variations (e.g. Unwin, 1980). Typically, cloudy and/or windy days reduce heat island magnitudes for a city.

Urbanization causes changes in the energy, moisture, and momentum systems, but few studies demonstrate pre–post urban climate conditions (Lowry, 1977). One excellent example is the experiment conducted to specifically illustrate how a city, as it developed from a rural environment, affected the local and regional climate (Landsberg, 1981). Most urban climate studies rely on geographic comparisons between the city and its surroundings in order to produce an estimate of the urban effect on local climate. Considerable attention has been given to the study of historical weather records in cities to evaluate temperature trends that are more urban in origin versus trends more attributable to global signals of change (e.g. global warming). A large number of stations with long records are needed for trend analyses, and many of the world's weather stations are in or near urban-affected locales. Thus, it is often difficult to decipher global change from such sites (e.g. Hansen, et al., 1999, 2001). Furthermore, placing typical weather stations in urban areas to study how cities alter climate is a most challenging endeavor in and of itself (Oke, 1999). This arises because of the complex structure of the urban atmosphere, processes operating at differing scales, and the resultant climate patterns in the city (see Figure U1, after Oke, 1998).

Table U2 Urban climate effects for a mid-latitude city with about 1 million inhabitants (values for summer unless otherwise noted)

Variable	Change	Magnitude/comments
Turbulence intensity	Greater	10–50%
Wind speed	Decreased	5–30% at 10 m in strong flow
	Increased	In weak flow with heat island
Wind direction	Altered	1–10 degrees
UV radiation	Much less	25–90%
Solar radiation	Less	1–25%
Infrared input	Greater	5–40%
Visibility	Reduced	
Evaporation	Less	About 50%
Convective heat flux	Greater	About 50%
Heat storage	Greater	About 200%
Air temperature	Warmer	1–3°C per 100 years; 1–3°C annual mean up to 12°C hourly mean
Humidity	Drier	Summer daytime
	More moist	Summer night, all day winter
Cloud	More haze	In and downwind of city
	More cloud	Especially in lee of city
Fog	More or less	Depends on aerosol and surroundings
Precipitation		
Snow	Less	Some turns to rain
Total	More?	To the lee of rather than in city
Thunderstorms	More	
Tornadoes	Less	

Source: Adapted after Oke (1997), p. 275.

Methods of evaluating urban climate

Many methods are used to determine how a city affects climate. Early methodologies included sampling the differences between urban–rural environments, upwind–downwind portions of the urban area, urban–regional ratios of various climatic variables, time trends of differences and ratios, time segment differences such as weekday versus weekend, and point sampling in mobile surveys throughout the urban environment (Lowry, 1977). Much of this sampling led to the discovery of the famous heat-island phenomenon.

Methodological inadequacies of many of the early studies have been pointed out in recent decades, and accurate time-series data remain a problem of analysis (Lowry, 1977; myriad studies on filtering out urban effects to reveal global trends). These inadequacies led to increased studies of processes involved, particularly fluxes of energy, moisture, and momentum in urban environments. Process studies help to provide a better characterization of how urbanization alters the surface–atmospheric system (Oke, 1979). Much attention has been given to internal variability of climate conditions within the urban environment and to the importance of the UCL (Arnfield, 1982; Grimmond, 1992; Grimmond and Oke, 1995, 1999; Johnson and Watson, 1984; Oke, 1981).

The urban heat island

Cities, no matter what their size, tend to be warmer than their surroundings. One can observe this biking through the urban landscape (Melhuish and Pedder, 1998). This fact was discovered by scientists well over a century ago (e.g. Howard, 1833), and is well known as evidenced by its mention in virtually every book on modern climatology and ecology (e.g. Thompson and Perry, 1997; Bonan, 2002). Since cities are regional agglomerations of people, buildings, and urban activities, they are spots on the broader, more rural surrounding land. These spots produce a heat-island effect on the spatial temperature distribution in an area (see Figures U7a and b in the later section on remote sensing).

The reasons for heat-island formation are many-fold (Table U3 after Oke, 1979). City size, morphology, land-use configuration, and geographic setting (e.g. relief, elevation, regional climate) dictate the intensity of the heat island, its geographic extent, orientation, and its persistence through time. Oke (1981) illustrates the effect of city size (as indicated by population size) on the maximum urban heat-island intensity (see Figure U2). Although population is only a surrogate measure for many of the causes of a heat island, there is a significant correlation

indicated, and population serves as a useful reference for expected heat-island formation.

In evaluating the heat-island intensity of cities, several cautionary notes must be emphasized. The method of sampling and/or the accuracy of historical weather records from available rural and urban locales must be carefully considered (Oke, 1999). Much of the earlier work in heat-island detection is of somewhat limited value due to non-specification of probable pre-urban conditions in an area, and biases in spatial sampling of the extent of the heat island (Lowry, 1977; Landsberg, 1981). Numerical adjustments of historical temperature records must be considered by the urban researcher, since available data may be biased (e.g. observation time of various stations may be different) and influences of local changes in station locations on temperature and precipitation statistics may go undetected (e.g. Winkler and Skaggs, 1981). The more process-oriented urban climatic studies in the last two decades are not only providing measures of explanation of the heat-island phenomenon, but also are allowing for a better understanding of the efficacy of the earlier, more descriptive studies of the urban heat island.

Table U3 Mechanisms hypothesized to cause the urban heat island effect

- Urban Boundary Layer
  - Anthropogenic heat from roofs and stacks
  - Entrainment of air scoured from warmer canopy layer
  - Entrainment of heat from overlying stable air by the process of penetrative convection
  - Shortwave radiative flux convergence within polluted air
- Urban Canopy Layer
  - Anthropogenic heat from building sides
  - Greater shortwave absorption due to canyon geometry
  - Decreased net longwave loss due to reduction of sky view factor by canyon geometry
  - Greater daytime heat storage (and nocturnal release) due to thermal properties of building materials
  - Greater sensible heat flux due to decreased evaporation resulting from removal of vegetation and surface waterproofing
  - Convergence of sensible heat due to reduction of wind speed in the canopy

Source: After Oke (1979).

Radiation and energy balance of the city

Shortwave radiation

An urban area affects the exchanges of shortwave and longwave radiation by air pollution and complex changes of surface radiative characteristics. Figure U3 illustrates radiative fluxes and processes in a city atmospheric system and the profiles of shortwave radiative heating and longwave radiative cooling due to the existence of an urban aerosol layer. The attenuation of incoming shortwave radiation (fluxes 2 and 4 divided by 1; see Figure U3) has been analyzed in numerous urban climatic environments. It is thought that the attenuation in the city is 2–10% more than in the country. Generally, the ultraviolet portion of the electromagnetic spectrum (< 0.4 μm), the so-called UV, is depleted by as much as 50% (e.g. Petersen et al., 1978). However, total depletion across all solar wavelengths (0.15–4.0 μm) is much smaller, less than 10% (Petersen and Flowers, 1977; Petersen and Stoffel, 1980). The processes of scattering and absorption, which account for the attenuation, require further study to predict their relative contribution to total shortwave radiation depletion.

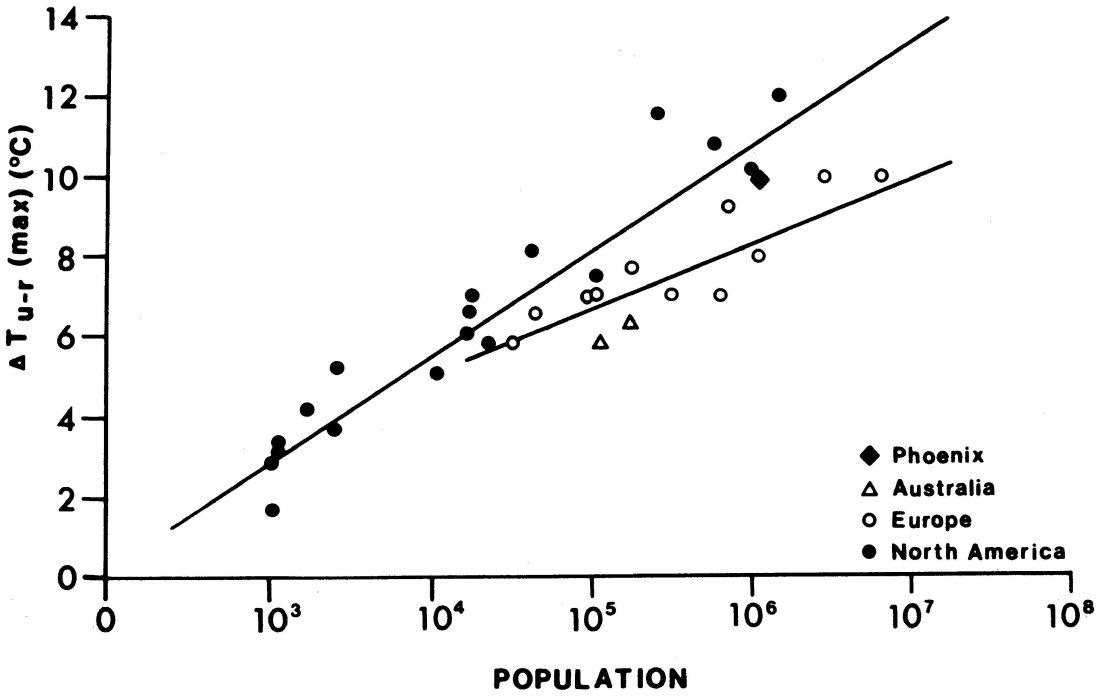

Figure U2 The maximum urban heat island intensity (ΔT_{u-r} [max]) versus population for 32 cities in Europe, North America, and Australia (data from Oke, 1981).

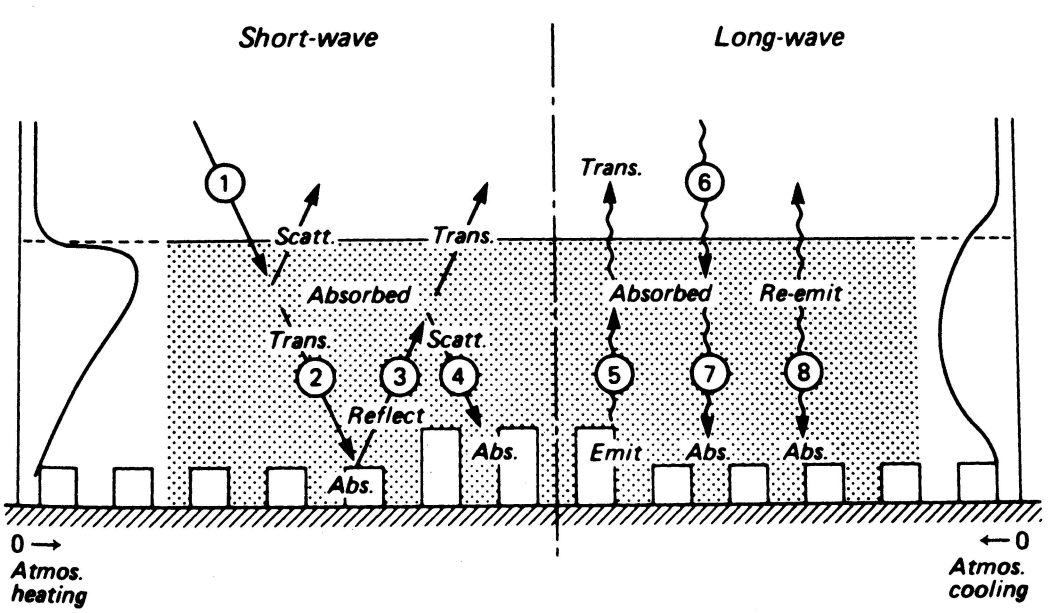

Figure U3 Radiative exchanges in a polluted urban boundary layer, including generalized profiles of shortwave radiative heating (left) and longwave cooling (right) due to the aerosol layer (shaded). Numbered fluxes are referred to in the text (after Atwater, 1971; Oke, 1982).

Albedo

The second major effect by the city is the change in the ratio of outgoing shortwave radiation (flux 3) to that of incident shortwave radiation at the complex, three-dimensional city interface (fluxes 2 and 4). This ratio, the albedo, is typically less in urban areas than in the surrounding landscape. Lower albedoes are due to darker surface materials making up the urban landscape mosaic and also due to effects of trapping of shortwave radiation by the vertical walls and the urban canyon-like morphology. There is considerable variation of albedo within the city depending on the percent vegetative cover, building material variation and roof composition, and land-use characteristics (see Table U4).

The difference in albedo between a city and its environs depends also, of course, on the surrounding terrain. A city surrounded by dark forest may experience very little albedo difference from the forest cover (both may range from 10% to 20%). In winter a midlatitude to high-latitude city with surrounding snow cover may display a much lower albedo than its surroundings. Thus, since cities receive 2–10% less shortwave radiation than their surroundings, yet have slightly lower albedoes (by less than 10%), most cities experience very small overall differences in absorbed shortwave radiation from rural locations nearby.

Table U4 Albedo values of urban surface materials

Material	Albedo (%)
Concrete	27.1
Blacktop/asphalt	10.3
Brick, red	32.0
Brick, yellow/buff	40.0
Brick, white/cream	60.0
Glass	9.0
Paint, dark	27.5
Paint, white	68.7
Roofing shingles	25.0
Snow, weathered	55.0
Stone	31.7
Tar-gravel roof	13.5
Yard (90% lawn, 10% soil)	24.0

Source: Data from Arnfield (1982), p. 104.

Longwave radiation

Longwave radiation is affected by city pollution and the fact that most urban surface areas are warmer. Warmer surfaces promote greater thermal emission of energy vertically upward from the city surface compared to rural areas, particularly at night (flux 5). Some longwave radiation is reradiated by urban aerosols back to the surface and also from the warmer urban air layer (fluxes 7 and 8). Thus, increases in incoming longwave radiation and outgoing longwave radiation are usually experienced in urban areas (that is, fluxes 7 and 8 are greater than flux 6 would be at the urban surface).

It is thought that outgoing longwave radiation increases are slightly greater than the incoming increases in the city, again especially on clear, calm nights. During daytime there is little difference between the city and its surroundings. However, surface emissivity (amount emitted relative to black-body amounts for a given temperature) can be quite different between country and city areas, and can account for considerable longwave radiation variations (Yap, 1975). A major consideration is that in the city a three-dimensional surface temperature must be characterized to accurately estimate the flux values of radiation and the energy budget (e.g. Voogt and Oke, 1997, 1998).

Net all-wave radiation

Generally, variations in the shortwave and longwave radiation fluxes between a city and its environs are relatively small, and the net all-wave radiation (the balance between incoming and outgoing shortwave and longwave radiation) may actually be less in urban areas (e.g. in St Louis there is 4% less net radiation in the city; White et al., 1978). The exact differences depend on land use, city building density and arrangement, aerosol composition of the urban atmosphere and climate of the city surroundings, as well as other factors such as artificial heat emissions and the topography of the region. In the UCL, what is called the urban sky view factor (USVF) is decreased considerably below a totally unobstructed horizon. This latter condition is more typical of the countryside. An obstructed horizon consisting of structures that make up the UCL reduces radiative loss and can account for excess heat in the city (Oke, 1981). The emission of heat from the UCL structures has been hypothesized as explaining a city's heat-island intensity. Figure U4 shows a correlation of the UCL sky view factor with the maximum heat island intensity for 31 cities plotted in Figure U4. The USVF is specifically defined as:

$$\mathrm{USVF} = (1 - 2\mathrm{UWVF})$$

$$\mathrm{UWVF} = 0.5(\sin^2\theta + \cos\theta - 1)(\cos\theta)^{-1}$$

$$\theta = \tan^{-1}(H/0.5W)$$

where: H = height of UCL
W = width of the UCL.

Note the tightening of the correlation, indicating that for a given population, a European city has a more open geometry, whereas most US cities have deeper canyons in their core areas. The individual correlations of European–Australian and North American population versus maximum heat-island intensities now merge into one generalized correlation shown in Figure U4. Urban climatologists are increasingly using photographic and GIS methods to derive USVF variability within cities. Figures U5a and b illustrate results for downtown Salt Lake City for USVF and building heights (Brown and Grimmond, 2001).

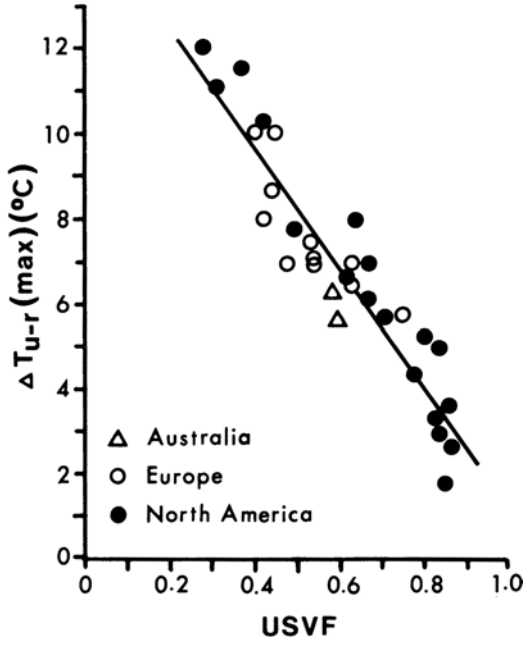

Figure U4 The maximum urban heat-island intensity (ΔT_{u-r} [max]) versus urban sky view factor (USVF) for 31 cities. The equation is ΔT_{u-r} (max) = −13.3 USVF + 14.86 (r^2 = 0.87, standard error of the estimate = 0.96°C).

Total energy balance

Not many long-term studies of a city's entire energy balance have been made (Oke, 1979). One specific reason relates to important paradigms in climatology, shifting only in the last five decades to considering physical principles of the energy, moisture and mass exchanges at the Earth–atmosphere interface (Miller, 1965). However, over the last decade, many cities worldwide have been studied through the use of tall towers with energy flux sensors, GIS, remote sensing and modeling procedures (e.g. Grimmond, 1992; Grimmond and Oke, 1995, 1999).

The city energy budget or balance can be simplified in Figure U6a to:

$$Q^* + Qf = Qe + Qh + \Delta Qs + \Delta Qa$$

where: Q^* = net all-wave radiation
= $K^* + L^*$ (net shortwave and longwave radiation)
Qf = anthropogenic heat emission ($Qfv + Qfh + Qfm$)
Qe = latent heat flux
Qh = sensible heat flux
ΔQs = net heat storage in the city
ΔQa = net advection into or out of the city.

Since Q^* is not that different between a city and its surroundings, the observed heating in cities is likely accounted for by Qf, (Qe, Qh), and ΔQs. Usually, ΔQa is negligible. The contribution of Qf to the total energy balance is highly city-dependent and seasonally variable. Qf ranges from nil to 300% of Q^*, depending on the degree of industrialization (Qf is high in more industrialized cities), latitude (Qf is high in higher-latitude cities), and season (Qf is higher in winter). Qf is composed of heat produced by combustion of vehicle fuels (Qfv), stationary source releases such as within buildings (Qfh), and heat released by metabolism (Qfm). Qfv is a function of type and amount of gasoline used, number of vehicles, distance traveled, and fuel efficiency. Qfh requires an analysis of consumer usage of fuel such as gas and electricity. Qfm can be evaluated by active and sleep rates. For people metabolic rates have been given (Oke, 1979). Bach (1970) suggests rates for animals.

Sensible, latent, and storage heat

The repartitioning of energy in urban areas among sensible, latent, and storage heat processes primarily depends on the mosaic of land uses in the city as compared to rural areas. Generally, the drier urban building and road materials induce higher Qh, less Qe, and higher ΔQs in urban areas. A term labeled Qg is specified in the energy budget equation often as part of ΔQs and is the soil heat flux. Significant Qe does occur in cities. This is theorized to be due to urban irrigation effects and vegetation in the city (Kalanda et al., 1980). Marotz and Coiner (1973) indicate that vegetation in urban areas is not as limited as supposed, and Oke (1978) shows that $\Delta Qs/Q^*$ ratios for rural areas vary by only about 0.10 from those for suburban and urban areas.

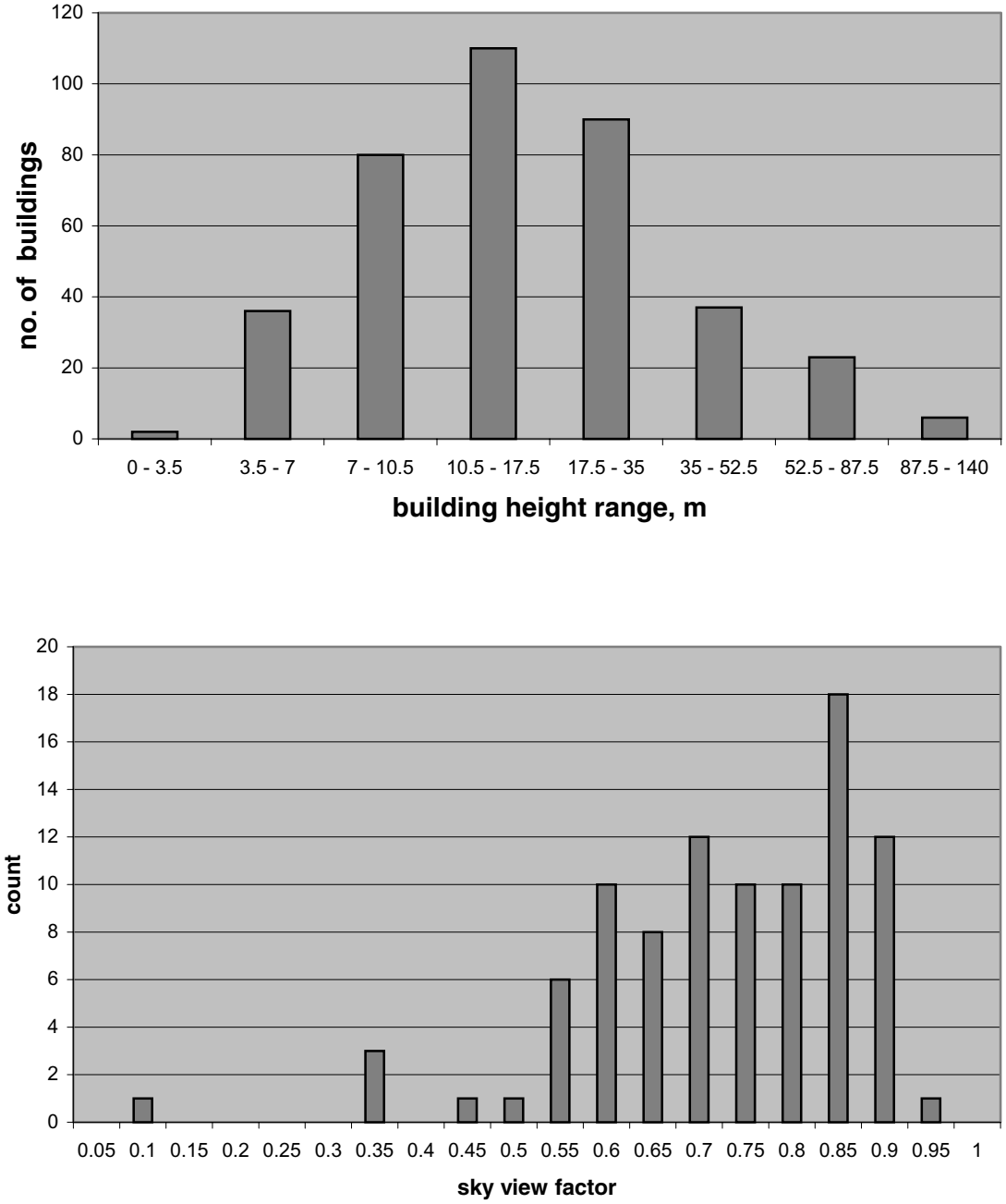

Figure U5 *Upper*: histogram of the computed sky view factor for street-level positions in downtown Salt Lake City. *Lower*: histogram of the building heights for downtown Salt Lake City (after Brown and Grimmond, 2001).

Table U5 shows some recent results for selected US cities after Grimmond and Oke (1995). Note the substantive fluxes of Q_h and ΔQ_s, also significant Q_e, especially for the more moist city of Chicago. In a detailed evapotranspiration study of nine places, Grimmond and Oke (1999) show that the ratio of Q_e/Q^* ranges from 0.09 (Mexico City with very little external water use) to Chicago's ratio of 0.46 (Table U5).

Goward (1981) lists thermal properties of typical interface materials, noting that urban area materials have similar thermal properties and that urban thermal inertias are higher than dry soils but lower than wet soils (see Table U6). Differences in UCL structure and composition are the keys to explaining heat excesses in cities, rather than just the thermal properties of city materials *per se*. Much research remains on this point, and has become a focal point in the field of urban climatology (Arnfield, 1982; Barring et al., 1985; Goldreich, 1985; Goward, 1981; Grimmond and Oke, 1995, 1999; Johnson and Watson, 1984; Oke, 1981, 1982; Terjung and O'Rourke, 1980).

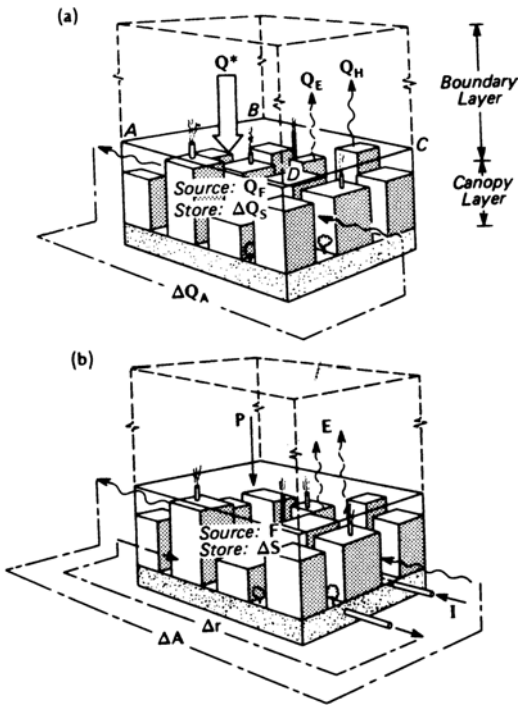

Figure U6 Schematic depiction of the fluxes involved in (**a**) the energy and (**b**) the water balance of an urban building air volume (after Oke, 1978, p. 242).

Table U5 Summary of daytime mean summer energy balance fluxes (MJ/m^2/day) for selected cities derived from tall tower observations (Grimmond and Oke, 1995).

Location	*Q**	*Qh*	*Qe*	Δ*Qs*	*Qg*
Tucson, AZ	16.27	7.54	4.11	4.62	Na
Sacramento, CA	12.65	5.19	3.79	3.67	12.73
Chicago, ILl	17.20	5.58	7.11	4.51	2.65
Los Angeles, CA	16.40	5.74	4.12	6.54	1.37

Remote sensing of urban surface temperature

The extreme land cover and spatial heterogeneity of the city landscape is problematic to the synoptic collection of *in-situ* measurements of energy balance flux parameters. Longwave radiation emitted upward from the urban surface (L^*), however, can be measured as a separate flux across the city landscape using thermal infrared (TIR) remote sensing. A number of investigators have provided evidence using TIR remote sensing data that urban areas are strong daytime longwave emitters (Rao, 1972; Pease and Nichols, 1976; Auer, 1978, Carlson and Boland, 1978; White et al., 1978; Roth et al., 1989). Other researchers have used remote sensing data to observe nighttime longwave radiation characteristics of cities (Dabberdt and Davis, 1974; Roth et al., 1989). As indicated by Table U6, however, the thermal properties of surfaces typical of the urban landscape are highly variable, and this variability is compounded even further by other factors, such as inconsistencies and deterioration caused by weathering or residue formation from automobiles. Flynn (1980), therefore, suggests that the problem related to the effects of surface material types and patterns on urban climatological phenomena, including the urban heat island effect, is a spatial one. A solution is to measure the attributes of space at a scale commensurate with that where the process becomes evident. The object of study then becomes the urban space that describes the energy budget or climatic processes within an areal unit. Flynn (1980) notes that approaching the problem in this way focuses on the pattern analysis and measurement of a basic urban surface (i.e. surface material type) and may explain some of the variability in urban temperatures across the city landscape. Thus, although TIR remote sensing data obtained from satellites are useful for discerning the general temperature characteristics of urban surfaces, these data must be obtained at spatial scales at which energy budgets for discrete surfaces material types can be identified (e.g. concrete, trees, rooftops, asphalt) to adequately quantify how thermal energy emanating from the composite urban landscape forces development of the urban heat island effect.

In this respect, high spatial resolution (i.e. <20 m) TIR remote sensing data have been shown to be extremely useful for measuring urban thermal energy balance characteristics (Quattrochi and Ridd, 1994, 1998; Lo et al., 1997; Quattrochi et al., 2000). For example, Figure U7a is a mosaic of individual

Table U6 Thermal properties of typical interface materials

Material	Thermal conductivity $W\,m^{-1}\,°C^{-1}$	Specific heat $J\,kg^{-1}\,°C^{-1} \times 10^3$	Density $kg\,m^{-3} \times 10^3$	Thermal admittance $J\,m^{-2}\,°C^{-1}$ $sec^{-1/2} \times 10^3$
Asphalt	0.7454	0.92	2.114	1.204
Brick	0.6910	0.84	1.970	1.067
Concrete	0.9338	0.67	2.307	1.185
Glass	0.8794	0.67	2.600	1.213
Granite	2.7219	0.67	2.600	2.176
Limestone	0.9338	0.92	1.650	1.182
Sand (dry)	0.3308	0.80	1.515	0.633
Wood	0.2094	1.38	0.500	0.377
Soil (wet)	2.4288	1.48	2.000	2.681
Soil (dry)	0.2513	0.80	1.600	0.567
Water (20°C)	0.5988	4.15	0.998	1.579
Air (20°C)	0.0251	1.01	1.001	0.056

Source: After Goward (1981), p. 24. *Note*: Thermal admittance is the square root of the product of the other three quantities.

flight lines of airborne TIR data acquired at a 10 m spatial resolution during the day in summertime over the Atlanta, Georgia, USA, central business district (CBD). Given these are TIR data, surfaces that emit high surface temperatures (i.e. exhibit a high thermal energy response) are depicted in white to very light gray tones on Figure U7a. On the other hand, surfaces that are comparatively low emitters of surface temperatures (and subsequently, exhibit lower thermal energy responses in relation to other surfaces) are represented as dark gray to black in tone in the figure. The A–A′ line in Figure U7a represents a transect centered on the Atlanta CBD and extending 5 km to the northwest and southeast of the CBD. There is a mixture of land covers along the transect that, in turn, is reflected in the fluctuations of temperatures along the graph given in Figure U7b. It may be seen in reference to Figures U7a and b that, in general, the residential land covers that inherently have more vegetation (e.g. trees, grass) are relatively cool (~ 20°C) as opposed to the surfaces in the CBD that have considerably less vegetation and are predominantly composed of pavements, rooftops and other impervious surfaces, exhibit considerably higher surface temperatures of approximately 35°C. Hence, these high spatial resolution TIR aircraft remote sensing data can be used to identify thermal energy responses from discrete urban surfaces to assist in more accurately measuring longwave energy upwelling from the city surface as a factor in the overall city landscape regime and, ultimately, in assessing their effects on urban climatology.

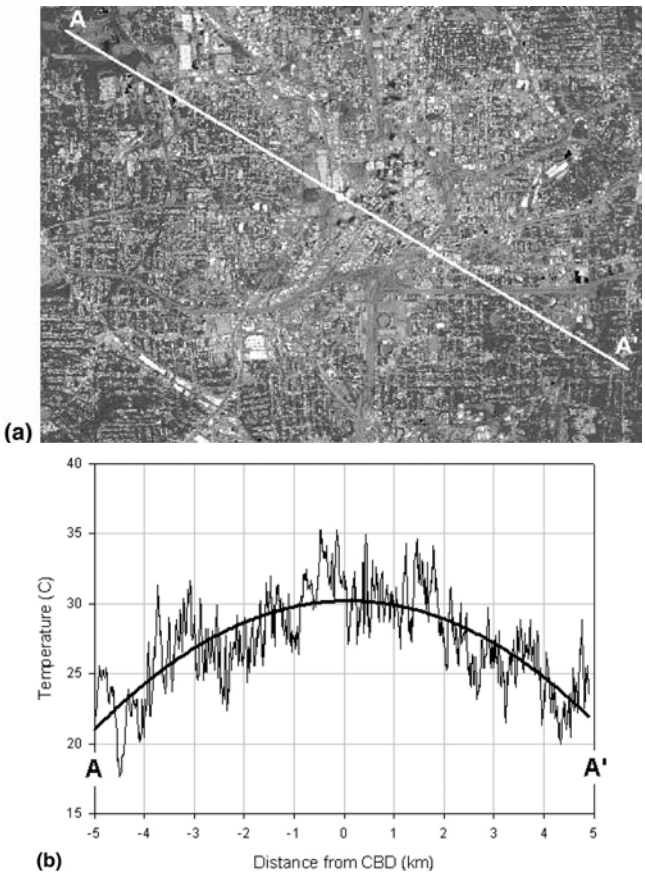

Figure U7 (**a**) Mosaic of individual flight lines of daytime airborne thermal infrared remote sensing data obtained over the Atlanta, Georgia, USA, central business district in summer. The A–A′ line represents a transect across the area to illustrate the variability in surface temperature energy responses across the Atlanta urban landscape (refer to **b**). (**b**) Graph of the mean surface temperature (solid line) across the Atlanta, Georgia, USA, central business district area as identified from daytime high-resolution TIR aircraft remote sensing data. Reproduced with permission, the American Society for Photogrammetry and Remote Sensing. Quattrochi, D.A., et al. "A Decision Support Information System for Urban Landscape Management Using Thermal Infrared Data." *Photogrammetric Engineering and Remote Sensing (PE&RS)*. October 2000: 1195–1207.

Moisture environment of cities

The processes of urbanization affect the surficial and atmospheric water budget. The water balance of an urban area is (Figure U6b):

$$p + I + F = E + \Delta r + \Delta S + \Delta A$$

where: p = precipitation
I = water supply from rivers and reservoirs
F = water released to air by combustion
E = evapotranspiration
Δr = net runoff
ΔS = moisture storage
ΔA = net moisture advection.

Precipitation

Many studies have shown that precipitation has appeared to have increased up to 30% in, and/or downwind of, large urban areas (e.g. Changnon, 1969; Dettwiller and Changnon, 1976; Atkinson, 1971). Stemming from Changnon's famous La Porte, Indiana, anomaly (1968) of increased precipitation downwind of the Chicago-Gary industrial area, much attention has been given recently to this subject. Detailed climatic investigations as part of the Metropolitan Meteorological Experiment (METROMEX) in St Louis, Missouri, have yielded estimates of urban effects on precipitation (Changnon et al., 1977; Ackerman et al., 1978; Changnon, 1981). Results indicate that summer is the time of maximum urban effect on precipitation (Figure U8) due to the dominance of convection. Analysis of rain cells, radar echo counts, detailed raingauge measurements, and temperature and wind field studies in and around St Louis have led to causal explanations of rainfall excesses that include: (1) pollution; (2) modification of the thermal structure of the UBL; and (3) deepening of the mixing layer and stronger vertical entrainment of heat and moisture in portions of the metropolitan area. A convergence zone over the city is set up by increased sensible heating. The city is aerodynamically rougher, has more pollution (condensation nuclei sources), causes more thermal and mechanical turbulence, and particularly affects convective cloud formation and precipitation. However, topographic settings of cities must be clearly understood relative to induced differences in precipitation receipt in the urban region, before causal explanations such as the above can be applied to other cities in different environments.

Sheppard et al. (2002) use the Tropical Rainfall Measuring Mission (TRMM) satellite's precipitation radar (PR) data to identify warm-season rainfall patterns in and around six selected cities in the southeast United States (Atlanta, Georgia; Montgomery, Alabama; Nashville, Tennessee; San Antonio, Waco, and Dallas, Texas). The results substantiated earlier

METROMEX findings of downwind increases in the rainfall of about 28% on average some 30–60 km downwind of the cities studied, and highlight the usefulness of satellite data to determine urban effects. Precipitation increases due to human influences may show cyclic behavior due to pollution effects, even at the weekly time scale, as suggested in a study of the regional pollution and precipitation enhancement toward end of workweeks on the Atlantic seaboard of the US (Cerveny and Balling, 1999). Table U7 illustrates results from several cities focusing on the fluxes of Qe relative to Q^* and the expression of water loss in millimeters per day, after Grimmond and Oke (1999).

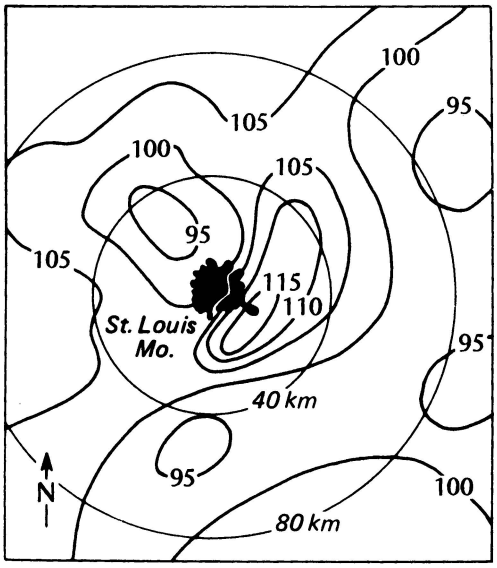

Figure U8 Average rural–urban ratios of summer rainfall in the St Louis area in the period 1949–1968. The rural–urban ratio is the ratio of the precipitation recorded at any station to that at two stations near the urban center (after Oke, 1978, p. 266).

Runoff

Since I and F are extra sources in cities, there is a net gain of moisture by urbanization. Water loss through E would be less in a city due to a waterproofing effect (Oke, 1980). The ΔS term would correspondingly be less. Assuming ΔA to be negligible, Δr would thus increase in cities. Indeed, many studies have indicated increased r in city environments, as well as changed hydrographic characteristics (e.g. Mather, 1978). There are four effects of land-use changes on the hydrology of the urban area: (1) peak flow is increased; (2) total runoff is increased; (3) water quality is lowered; and (4) hydrologic amenities – appearance of river channel and aesthetic impressions – are lowered (Mather, 1978).

Figure U9 illustrates two factors that control discharge characteristics before and after urbanization, shown here as a ratio related to percent impervious area and percent area served by storm sewers. These two factors are controls on the discharge of an area. Note that urban–preurban ratios of runoff increase as percent impervious surface area and percent storm sewers increase. Geographic information system processing of data is now used in hydrological studies, merged with simulation programs for stream flow analysis in urban areas (e.g. Brun and Band, 2000). In their work, relationships among runoff, base flow, impervious cover, and percent soil saturation for upper Gwynns Falls watershed, Baltimore, Maryland, were studied. It was possible to determine through modeling procedures the threshold percent impervious cover that would significantly alter runoff in the urbanizing watershed. In this case, current percent impervious surface cover is approximately 18%, whereas modeling suggests 20% is a threshold beyond which runoff alterations by land cover would significantly occur.

Humidity

Since E and ΔS are less, dewpoint is usually less in daytime in cities (e.g. Sisterson and Dirks, 1978; Brazel and Balling, 1986). At night a humidity island may result (e.g. Chandler, 1967; Kopec, 1973), due to extra E at night and contributions of F. Since recent studies have not shown Qe and E to be that

Table U7 Daily mean fluxes of Qe and water loss (E) for selected cities and conditions (after Grimmond and Oke, 1999)

Location[a]	Q^*	Qe	Qe/Q^*	E (mm.day)	P (mm/month)	P (mean monthly)	Practices[b]
C95	14.89	6.80	0.46	2.76	80.5	92.0	1
A93	13.74	4.93	0.36	2.00	0.0	0.0	2
T90	12.50	4.90	0.39	1.99	16.3	5.4	3
A94	15.58	4.70	0.30	1.94	0.0	0.0	4
Mi95	13.74	4.58	0.33	1.87	79.8	180.9	5
S91	9.72	4.38	0.45	1.77	0.0	1.8	6
Vs92	8.88	2.68	0.30	1.10	23.2	41.1	7
Sg94	12.45	3.46	0.28	1.40	0.0	0.25	8
Vl92	11.41	1.48	0.13	0.60	23.2	41.1	9
Me93	3.38	0.31	0.09	0.14	0.0	0.0	10

[a] In order, Chicago, ILl June/Aug 1995; Arcadia, CA July/Aug 1993; Tucson, AZ , June 1990; Arcadia, CA July 1994; Miami, FL, May/June 1995; Sacramento, CA, Aug 1991; Vancouver, BC, July/Sept, 1992; San Gabriel, CA, July, 1994; Vancouver, BC, Aug, 1992; Mexico City, D.F., Dec 1993.

[b] 1 = extensive irrigation; 2 = extensive irrigation (see A94); 3 = xeric landscaping; low water use vegetation, greenspace irrigated automatically at night/early a.m.; 4 = As A93. irrigation ~1.37 mm/day; 5 = frequent rainfall, also irrigation; 6 = irrigation on alternate days; 7 = irrigation ban − external use ~0.25 mm/day; 8 = As A93 but more hand watering, irrigation ~1.32 mm/day; 9 = irrigation ban in Vs92; 10 = some street washing, very little external use.

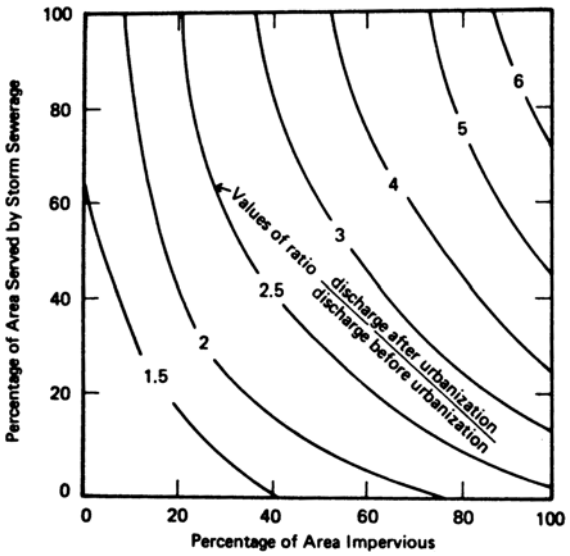

Figure U9 Two factors that cause increased discharge in the urban area as related to the ratio of discharge *after* urbanization to that *before* urbanization (after Mather, 1978).

different between city and surroundings, evaluations of F are important in the understanding of the humidity contrasts. Its absence may mean a negative humidity island in the city (drier); its presence a positive humidity island (wetter). Fog differences are not great between cities and rural areas although, due to pollution, cities have more haze, smog, and perhaps more slight fog. More cloud condensation nuclei and ice nuclei have been observed in cities, but knowledge is very unsatisfactory at this point about the effects on urban precipitation (Landsberg, 1981). Holmer and Eliasson (1999) report vapor pressure results between urban and rural areas for nine locations from previous studies plus their own study in Goteborg, Sweden. They identified an urban moisture excess, particularly at night, that also was related to the urban heat island and longwave radiative fluxes.

Air movement in cities

Urban areas affect air flow, both speed and direction, on micro- and meso-scales. The aerodynamic roughness of urban areas (level above the ground where wind speed becomes greater than zero on average) is larger by some 0.5–4.0 m than in rural areas, and the city therefore produces more frictional drag. A heat-island effect in cities influences the pressure field and also vertical stability of the air. This will affect local airflow. These effects also depend on overall gradient wind strength across the urban region. Many studies have shown that, as wind increases, the magnitude of the urban heat island diminishes.

Wind speeds

When regional air flow is strong, the aerodynamic roughness of the city is dominant and is important in inducing increases in mechanical turbulence on the order of 30–50% (Oke, 1980). Under light winds, air pressure differences and atmospheric stability effects, in addition to roughness, are critical in determining city wind speeds from place to place. The built

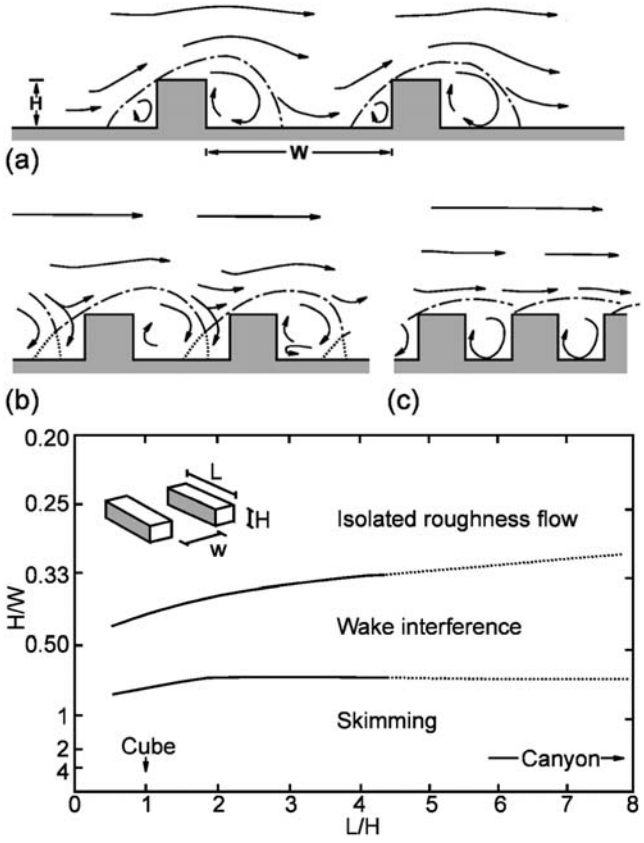

Figure U10 Threshold H/W ratios for the transition flow between flow regimes (**a**) skimming → wake interference; (**b**) wake interference → isolated roughness (from Hunter et al., 1992, used by permission of Pergamon Press Ltd).

environment affects the flow regimes of air through and over the city (Hunter et al., 1990). Generally, the length/height ratio and height/width ratio of buildings control the flow regime among isolated roughness flow, wake interference flow, and skimming flow (viewed in Figures U10a and b). Generally, under light regional flow, winds tend to accelerate in cities compared to rural areas because of strong rural atmospheric stability and the increased turbulence over the warmer, rougher city surface. Under strong flow, winds generally decelerate in the urban area due to greater frictional effects of the city on airflow. Studies have shown that there appears to be a critical regional flow speed separating the accelerating from decelerating wind response in the city (Chandler, 1965; Bornstein and Johnson, 1977; Lee, 1979). This speed, however, is quite variable and ranges from 0.8 to 5.6 m/s.

Wind direction

Wind direction differences in cities and in rural areas relate to frictional retardation effects. Decelerating winds will promote cyclonic turning toward lower pressure; accelerating winds produce anticyclonic turning (Ackerman, 1974; Angell and Bernstein, 1975; Lee, 1973). Wind direction changes induced by a city also vary diurnally in relation to the depth of the mixing layer. During the day the turning effect lessens, whereas at night it reaches a maximum.

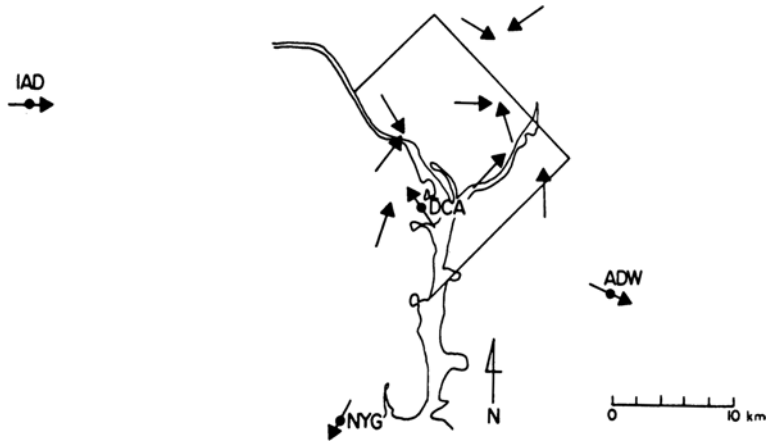

Figure U11 Wind convergence on a hot summer afternoon toward the city of Washington, DC. IAD = Dulles International Airport; DCA = Washington National Airport; ADW = Andrews Air Force Base; and NYG = Quantico Marine Base (after Landsberg, 1981, p. 135).

Urban circulations, much like the classic sea breeze, have been documented in addition to being theorized from laws of thermodynamics (Bach, 1970; Hjelmfelt, 1982; Shreffler, 1978; Vukovich and King, 1980). Landsberg (1981) illustrates the summer air circulation for Washington, DC (Figure U11). Note the convergence locally in the city boundary. Other air flow systems, such as synoptic fronts and sea breezes, also can be affected by cities. Manhattan, New York, for example, slows cold frontal passages upwind of the city and speeds them up downwind, especially when a strong heat island prevails (Loose and Bornstein, 1977). Wind conditions at street level and in the UCL are very complex and relate to physical barriers, building sizes, orientations, building densities, and general land-use patterns. As a generalization, winds are slowed in the UCL. However, effects of wind channeling and funneling can occur, depending on prevailing winds and the overall orientation and morphology of the city landscape.

Conclusions

The climate of cities will continue to be of importance to the ever-expanding urban population of the world. The application of research findings of urban climatology in building designs and urban environmental planning is beginning to emerge but is not yet widespread (Bonan, 2002). Due to the complexity of the urban landscape and the variability of dimensions, land use, morphology, and other characteristics, much research still remains on just how a city affects the surface and atmospheric climatic environment, and the city's overall urban ecology. Equally, if not more important, are the interactions of the city climate system with other elements of the entire urban ecosystem (Douglas, 1981; Bonan, 2002). The discovery of these interrelationships will eventually aid in planning solutions related to pollution, health, comfort, water supplies, and general quality of life among urban dwellers.

Anthony J. Brazel and Dale Quatrocchi

Bibliography

Ackerman, B., 1974. Wind fields over St. Louis in undisturbed weather. *American Meteorological Society Bulletin*, **55**: 93–95.

Ackerman, B.S., Changnon, S.A., Dzurisin, G., et al., 1978. *Summary of METROMEX*, vol. 2: *Causes of Precipitation Anomalies*. Bulletin 63. Urbana, IL: Illinois State Water Survey.

Angell, J.K., and Bernstein, A.B., 1975. Flow across an urban area determined from double-theodolite pilot balloon observations. *Journal of Applied Meteorology*, **14**: 1072–1079.

Arnfield, A.J., 1982. An approach to the estimation of the surface radiative properties and radiation budget of cities. *Physical Geography*, **3**(2): 97–122.

Atkinson, B.W., 1971. The effect of an urban area on the precipitation from a moving thunderstorm. *Journal of Applied Meteorology*, **10**: 47–55.

Atwater, M.A., 1971. The radiation budget for polluted layers of the urban environment. *Journal of Applied Meteorology*, **10**: 205–214.

Auer, A.H., Jr, 1978. Correlation of land use and cover with meteorological anomalies. *Journal of Applied Meteorology*, **17**: 636–643.

Bach, W., 1970. An urban circulation model, *Archiv für Meteorologie, Geophysik, und Bioklimatologie*, **B18**: 155–168.

Barring, L., Mattsson, J.O., and Lindqvist, S., 1985. Canyon geometry, street temperatures, and urban heat island in Malmo. Sweden. *Journal of Climatology*, **5**: 433–444.

Beryland, M.E., and Kondratyev, K.Ya., 1972. *Cities and the Global Climate* (A. Nurklik, trans.). Downsview, Ontario: Atmospheric Environment Service.

Bonan, G.B., 2002. *Ecological Climatology Concepts and Applications*. Cambridge: Cambridge University Press.

Bornstein, R.D., and Johnson, D.S., 1977. Urban–rural wind velocity differences. *Atmosphere and Environment*, **1**: 597–604.

Brazel, A.J., 1987. Urban climatology. In Oliver, J., and Fairbridge, R.W., eds., *Encyclopedia of Earth Sciences*, vol. XI: *Encyclopedia of Climatology*. New York: Van Nostrand Reinhold, pp. 889–901.

Brazel, S.W., and Balling, R.C., Jr, 1986. Temporal analysis off long-term atmospheric moisture levels in Phoenix, Arizona. *Journal of Climatology and Applied Meteorology*, **25**: 112–117.

Brown, M.J., and Grimmond, S., 2001. Sky view factor measurements in downtown Salt Lake City. Data report for the DOE CBNP URBAN Experiment, October 2000, Los Alamos National Laboratory, New Mexico, LA-UR-01-1424.

Brun, S.E., and Band, L.E., 2000. Simulating runoff behavior in an urbanizing watershed, Computers. *Environment and Urban Systems*, **24**: 5–22.

Carlson, T.N., and Boland, F.E., 1978. Analysis of urban-rural canopy using a surface heat flux/temperature model. *Journal of Applied Meteorology*, **17**: 998–1013.

Cerveny, R.S. and Balling, R.C., Jr, 1999. Identification of anthropogenic weekly cycles in Northwest Atlantic pollution, precipitation, and tropical cyclones. *Nature*, **394**: 561–562.

Chandler, T.J., 1965. *The Climate of London*. London: Hutchinson.

Chandler, T.J., 1967. Absolute and relative humidities in towns. *American Meteorological Society Bulletin*, **48**: 394–399.

Chandler, T.J., 1976. *Urban Climatology and Its Relevance to Urban Design*. Technical Note 149. Geneva: World Meteorological Organization.

Changnon, S.A., Jr, 1969. Recent studies of urban effects on precipitation in the United States. *American Meteorological Society Bulletin*, **50**: 411–421.

Changnon, S.A., Jr, 1981. METROMEX: a review and summary. *Meteorological Monographs* **40**: 1–181.

Changnon, S.A., Jr, 1983. Purposeful and accidental weather modification: our current understanding. *Physical Geography*, **4**(2): 126–139.

Changnon, S.A., Huff, F.A., Schickedanz, P.T., and Vogel, J.L., 1977. *Summary of METROMEX, vol. 1: Weather Anomalies and Impacts*. Bulletin 62. Urbana, IL: Illinois State Water Survey.

Dabberdt, W.F., and Davis, P.A., 1974. *Determination of Energetic Characteristics of Urban–Rural Surfaces in the Greater St Louis Area*. US Environmental Protection Agency project report, April, Washington, DC, USA.

De Dear, R.J., Kalma, J.D., Oke, T.R., and Auliciems, A., 2000. Biometeorology and urban climatology at the turn of the millennium. Selected papers from the conference ICB-ICUC '99 (Sydney, 8–12 November 1999), WCASP-50, WMO/TD-No. 1026.

Dettwiller, J.W., and Changnon, S.A., Jr, 1976. Possible urban effects on maximum daily rainfall at Paris, St. Louis, and Chicago. *Journal of Applied Meteorology*, **15**: 517–519.

Douglas, I., 1981. The city as an ecosystem. *Progress in Physical Geography*, **5**(3): 315–367.

Flynn, J.J., 1980. Point pattern analysis and remote sensing techniques applied to explain the form of the urban heat island. Doctoral dissertation, State University of New York, College of Environmental Science and Forestry, Syracuse, New York.

Goldreich, Y., 1985. The structure of the ground-level heat island in a central business district. *Journal of Climatology and Applied Meteorology*, **24**(11): 1237–1244.

Goward, S.N., 1981. Thermal behavior of urban landscapes and the urban heat island. *Physical Geography*, **2**(1): 19–33.

Grimmond, C.S.B., 1992. The surburban energy balance: methodological considerations and results for a mid-latitude west coast city under winter and spring conditions. *International Journal of Climatology*, **12**: 481–497.

Grimmond, C.S.B. and Oke, T.R., 1995. Comparison of heat fluxes from summertime observations in the suburbs of four North American cities. *Journal of Applied Meteorology*, **34**(4): 873–889.

Grimmond, C.S.B., and Oke, T.R., 1999. Evapotranspiration rates in urban areas. In *Impacts of Urban Growth on Surface Water and Groundwater Quality* (Proceedings of IUGG 99 Symposium HS5, Birmingham, July 1999), IAHS Publication no. 259, pp. 235–243.

Hansen, J., Ruedy, R., Glascoe, J., and Sato. M., 1999. GISS analysis of surface temperature change. *Journal of Geophysical Research*, **104**(D24): 30 997–31 022.

Hansen, J., Ruedy, R., Sato, M., et al., 2001. A closer look at United States and global surface temperature change. *Journal Geophysical Research*, **106**(D20): 23 947–23, 963.

Hjelmfelt, M.R., 1982. Numerical simulation of the effects of St. Louis on mesoscale boundary-layer airflow and vertical air motion: simulations of urban vs. non-urban effects. *Journal of Applied Meteorology*, **21**: 1239–1257.

Holmer, B. and Eliasson, I., 1999. Urban–rural vapour pressure differences and their role in the development of urban heat islands. *International Journal of Climatology*, **19**: 989–1009.

Howard, L., 1833. *The Climate of London*, vols. 1–3. London: Harvey & Darton.

Hunter, I., Watson, I.D., and Johnson, G.T., 1990/1991. Modelling air flow regimes in urban canyons. *Energy and Buildings*, **15–16**: 315–324.

Johnson, G.T., and Watson, I.D., 1984. The determination of view-factors in urban canyons, *Journal of Climatology and Applied Meteorology*, **23**(2): 329–335.

Kalanda, B.D., Oke, T.R., and Spittlehouse, D.L., 1980. Suburban energy balance estimates for Vancouver, B.C. using the Bowen ratio-energy balance approach. *Journal of Applied Meteorology*, **19**: 791–802.

Kopec, R.J., 1973. Daily spatial and secular variations of atmospheric humidity in a small city. *Journal of Applied Meteorology*, **12**: 639–648.

Landsberg, H.E., 1981. *The Urban Climate*. New York: Academic Press.

Lee, D.O., 1973. Urban influence on wind directions over London. *Weather*, **32**: 162–170.

Lee, D.O., 1979. The influence of atmospheric stability and the urban heat island on urban-rural wind speed differences. *Atmosphere and Environment*, **13**: 1175–1180.

Lee, D.O., 1984. Urban climates. *Progress in Physical Geography*, **8**(1): 1–31.

Lo, C.P., Quattrochi, D.A., and Luvall, J.C., 1997. Application of high-resolution thermal infrared remote sensing and GIS to assess the urban heat island effect. *International Journal of Remote Sensing*, **18**: 287–304.

Loose, T., and Bornstein, R.D., 1977. Observations of mesoscale effects on frontal movement through an urban area. *Monthly Weather Review*, **105**(5): 563–571.

Lowry, W.P., 1977. Empirical estimation of urban effects on climate: a problem analysis. *Journal of Applied Meteorology*, **16**: 129–135.

Marotz, G.A., and Coiner, J.C., 1973. Acquisition and characterization of surface material data for urban climatological studies. *Journal of Applied Meteorology*, **12**: 919–923.

Mather, J.R., 1978. *The Climatic Water Budget in Environmental Analysis*. Lexington, MA: Lexington Books.

Melhuish, E., and Pedder, M., 1998. Observing an urban heat island by bicycle. *Weather*, **53**(4): 121–128.

Miller, D.H., 1965. The heat and water budget of the Earth's surface. *Advances in Geophysics*, **11**: 175–302.

Oke, T.R., 1974. *Review of Urban Climatology 1968–1973*. Technical Note 134. Geneva: World Meteorological Organization.

Oke, T.R., 1979. *Review of Urban Climatology 1973–1976*. Technical Note 169. Geneva: World Meteorological Organization.

Oke, T.R., 1980. Climatic impacts of urbanization. In Bach, W., Pankrath, J., and Williams, J., eds., *Interactions of Energy* and *Climate*. Boston, MA: Reidel, pp. 339–356.

Oke, T.R., 1981. Canyon geometry and the nocturnal urban heat island: comparison of scale model and field observations. *Journal of Climate*, **1**: 237–254.

Oke, T.R., 1982. The energetic basis of the urban heat island. *Royal Meteorological Society Quarterly Journal*, **108**(455): 1–24.

Oke, T.R., 1987. *Boundary Layer Climates.* London: Methuen.

Oke, T.R., 1997. Urban climates and global environmental change. In Thompson, R.D., and Perry, A.H., eds. *Applied Climatology: Principles and Practice*. London: Rutledge, pp. 273–287.

Oke, T.R., 1998. Observing weather and climate. *Proceedings of the Technical Conference on Meteorology and the Environment*. Instruments and Methods of Observation, Instruments and Observing Methods Report No. 70, WMO/TD-No. 877, WMO, Geneva, pp. 1–8.

Oke, T.R., 1999. Observing urban weather and climate using 'standard' stations. In De Dear, R.J., Kalma, J.D., Oke, T.R., and Auliciems, A., eds., *Biometeorology and Urban Climatology at the Turn of the Millennium*. Selected papers from the conference ICB-ICUC '99 (Sydney, 8–12 November 1999), WCASP-50, WMO/TD-No. 1026, pp. 443–448.

Pease, R.W., and Nichols, D.A., 1976. Energy balance maps from remotely sensed imagery. *Photogrammetric Engineering and Remote Sensing*, **42**: 1367–1373.

Petersen, J.T., and Flowers, E.C., 1977. Interaction between air pollution and solar radiation. *Solar Energy*, **19**: 23–32.

Petersen, J.T., and Stoffel, T.L., 1980. Analysis of urban-rural solar radiation data from St. Louis, Missouri. *Journal of Applied Meteorology*, **19**: 275–283.

Petersen, J.T., Flowers, E.C., and Rudisill, J.H., 1978. Urban–rural solar radiation and atmospheric turbidity measurements in the Los Angeles basin. *Journal of Applied Meteorology*, **17**: 1595–1609.

Quattrochi, D.A., and Ridd, M.K., 1994. Measurement and analysis of thermal energy responses from discrete urban surfaces using remote sensing data. *International Journal of Remote Sensing*, **15**: 1991–2022.

Quattrochi, D.A., and Ridd, M.K., 1998. Analysis of vegetation within a semi-arid urban environment using high spatial resolution airborne thermal infrared remote sensing data. *Atmosphere and Environment*, **32**: 19–33.

Quattrochi, D.A., Luvall, J.C., Rickman, D.L., Estes, M.G., Jr, Laymon, C.A., and Howell, B.F., 2000. A decision support system for urban landscape management using thermal infrared data. *Photogrammetric Engineering and Remote Sensing*, **66**: 1195–1207.

Rao, P.K., 1972. Remote sensing of urban heat islands' from an environmental satellite. *American Meteorological Society Bulletin*, **50**: 522–528.

Roth, M., Oke, T.R., and Emery, W.J., 1989. Satellite-derived urban heat islands from three coastal cities and the utilization of such data in urban climatology. *International Journal of Remote Sensing*, **10**: 1699–1720.

Shepperd, J.M., Pierce, H., and Negri, A.J., 2002. Rainfall modification by major urban areas: observations from spaceborne rain radar on the TRMM satellite. *Journal of Applied Meteorology*, **41**: 689–701.
Shreffler, J.H., 1978. Detection of centripetal heat-island circulations from tower data in St. Louis. *Boundary-Layer Meteorology*, **15**: 229–242.
Sisterson, D.L., and Dirks, B.A., 1978. Structure of the daytime urban moisture field. *Atmosphere and Environment*, **12**: 1943–1949.
Terjung, W.H., and O'Rourke, P.A., 1980. Simulating the causal elements of urban heat islands. *Boundary-Layer Meteorology*, **19**: 93–118.
Thompson, R.D., and Perry, A.H., 1997. *Applied Climatology: principles and practice*. London: Rutledge.
Unwin, D.J., 1980. The synoptic climatology of Birmingham's urban heat island 1965–1974. *Weather*, **35**: 43–50.
Voogt, J.A., and Oke, T.R., 1997. Complete urban surface temperatures. *Journal of Applied Meteorology*, **36:** 1117–1132.
Voogt, J.A,. and Oke, T.R., 1998. Radiometric temperatures of urban canyon walls obtained from vehicle traverses. *Theoretical and Applied Climatology*, **60**: 199–217.
Vukovich, F.M., and King, W.J., 1980. A theoretical study of the St. Louis heat island: comparisons between observed data and simulation results on the urban heat island circulation. *Journal of Applied Meteorology*, **19**(7): 761–770.
White, J.M., Eaton, F.D., and Auer, A.H., Jr, 1978. The net radiation budget of the St. Louis metropolitan area. *Journal of Applied Meteorology*, **17**: 593–599.
Winkler, J.A., and Skaggs, R.H., 1981. Effect of temperature adjustments on the Minneapolis–St. Paul urban heat island. *Journal of Applied Meteorology*, **20**: 1295–1300.
World Meteorological Organization, 1970. *Urban Climates*. Technical Note 108, No. 254, TP 141. Geneva: World Meteorological Organization.
Yap, D., 1975. Seasonal excess urban energy and the nocturnal heat island—Toronto. *Archiv für Meteorologie, Geophysik, und Bioklimatologie*, **B23**: 69–80.

Cross-references

Air Pollution Climatology
Bioclimatology
Energy Budget Climatology
Local Climatology
Microclimatology
Water Budget Analysis